AN EFFICIENT WAVELET-BASED ALGORITHM FOR IMAGE SUPERRESOLUTION

Nhat Nguyen

Scientific Computing and
Computational Mathematics Program
Gates Bldg. 2B
Stanford, CA 94305
nguyen@sccm.stanford.edu

Peyman Milanfar

Department of Electrical Engineering
University of California, Santa Cruz
Santa Cruz, CA 95064
milanfar@cse.ucsc.edu

ABSTRACT

Superresolution produces high quality, high resolution images from a set of degraded, low resolution frames. We present a new and efficient wavelet-based algorithm for image superresolution. The algorithm is a combination of interpolation and restoration processes. Unlike previous work, our method exploits the interlaced sampling structure in the low resolution data. Numerical experiments and analysis will demonstrate the effectiveness of our approach and illustrate why computational complexity only doubles for 2-D superresolution versus 1-D case.

1. INTRODUCTION

Figure 1 illustrates the superresolution setup. We are given three 4×4 pixels low resolution (LR) frames on an 8×8 high resolution (HR) grid, and we would like to obtain estimates of the original image on the HR grid. Each symbol (square, circle, triangle) indicates the sampling points of a frame with respect to the HR grid. We pick an arbitrary frame as a reference frame; in this case, the frame marked by the circular symbols. The sampling grid for the triangular frame is just a simple translation of the reference frame grid. The motion between the sampling grid for the square frame and the reference frame grid include translational, rotational, and magnification (zoom) components.

The forward relationship between a degraded, LR frame and the ideal HR image can be described as follows [2]:

$$\mathbf{f}_k = DCE_k\mathbf{x} + \mathbf{n}_k, \quad 1 \le k \le p, \qquad (1)$$

where D is the down-sampling operator, C is the blurring/averaging operator, E_k's are the affine transforms which map the HR grid coordinate system to the LR grid systems, $\mathbf{x}$ is the unknown ideal HR image, and
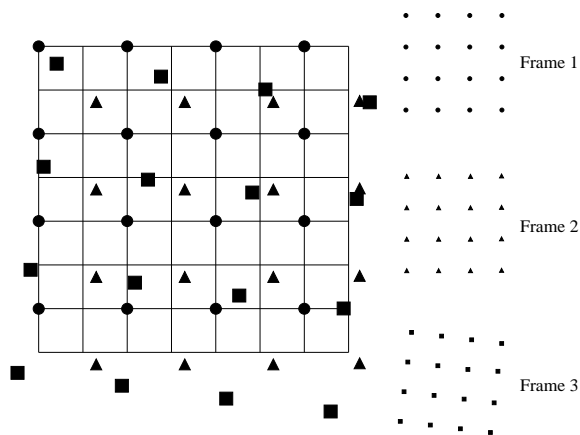

Figure 1: Low-resolution data on a high-resolution grid.

$\mathbf{n}_k$'s are the additive noise vectors. The LR frames $\mathbf{f}_k$ are given, and the decimation operator D is known. In this paper, we assume that C is spatially linear shift invariant, frame to frame motion and blurring parameters are known a priori or have been estimated (cf. [6]) from given data, and that frame to frame motion is purely translational or has been corrected to be so.

The shift invariance property allows the operators C and E_k to commute. Hence, (1) can be rewritten as

$$\mathbf{f}_k = DE_kC\mathbf{x} + \mathbf{n}_k, \quad 1 \le k \le p, \qquad (2)$$

Equation (2) motivates our two-step approach to superresolution. First, using the LR data frame samples $\mathbf{f}_k$, $1 \le k \le p$, we interpolate for $C\mathbf{x}$, the blurred version of the original HR image. Next, we deconvolve the blur C to obtain an estimate for $\mathbf{x}$. The rest of the paper will mostly address the interpolation step of the algorithm. Unlike previous interpolation-restoration superresolution algorithms [8, 9, 7], our interpolation

technique takes advantage of the inherent structure and regularity in the sampled data. Section 2 describes our interpolation method for 2-D interlaced data. Our algorithm is an extension of Ford and Etter [3] for interlaced sampling. Section 3 analyzes the computational complexity for the method. Experimental results with Forward Looking Infrared (FLIR) images are discussed in Section 4.

2. WAVELET INTERPOLATION OF INTERLACED 2-D DATA

Following work by Mallat [5], any image $f(t,s) \in L^2(\mathbf{R}^2)$ can be represented in terms of a separable, orthonormal basis generated by special scaling and wavelet functions $\phi(t)$ and $\psi(t)$. The basis functions are products of dilations and translations of $\phi(t)$ and $\psi(t)$, $\phi_{j,k}(t) \equiv 2^{j/2}\phi(2^j t - k)$, $\psi_{j,k}(t) \equiv 2^{j/2}\psi(2^j t - k)$. We have the following decomposition at scale J

$$
\begin{aligned}
f(t,s) \quad = \quad & \sum_{k,l \in \mathbf{Z}} a_{J,k,l}\phi_{J,k}(t)\phi_{J,l}(s) + \\
& \sum_{j \geq J}\sum_{k,l \in \mathbf{Z}} b^h_{j,k,l}\psi_{j,k}(t)\phi_{j,l}(s) + \\
& \sum_{j \geq J}\sum_{k,l \in \mathbf{Z}} b^v_{j,k,l}\phi_{j,k}(t)\psi_{j,l}(s) + \\
& \sum_{j \geq J}\sum_{k,l \in \mathbf{Z}} b^d_{j,k,l}\psi_{j,k}(t)\psi_{j,l}(s), \quad (3)
\end{aligned}
$$

with

$$
\begin{aligned}
a_{J,k,l} &= \iint f(t,s)\phi_{J,k}(t)\phi_{J,l}(s)dtds \\
b^h_{J,k,l} &= \iint f(t,s)\psi_{j,k}(t)\phi_{j,l}(s)dtds \\
b^v_{J,k,l} &= \iint f(t,s)\phi_{j,k}(t)\psi_{j,l}(s)dtds \\
b^d_{J,k,l} &= \iint f(t,s)\psi_{j,k}(t)\psi_{j,l}(s)dtds.
\end{aligned}
$$

In image superresolution, the data frames are given low resolution rectangular grids of sample points. Let h, w denote the height and width (in units of pixels) of a low resolution frame and r the resolution enhancement factor. The set of available data is then

$$
\begin{aligned}
& \{f(pr + \epsilon_{i_t}, qr + \epsilon_{i_s})\}, \\
& 0 \leq \epsilon_{i_t}, \epsilon_{i_s} < r, \quad p = 0, ..., h-1, \\
& q = 0, ..., w-1, \quad i = 1, ..., n.
\end{aligned}
$$

From these nhw sample points on low resolution grids, we would like to reconstruct values of $f(t,s)$ on high resolution grid points $\{(t,s)| \ t = 0, ..., hr-1, \ s = 0, ..., wr-1\}$. We substitute in sample values of $f(t,s)$

to obtain a set of linear equations. Ignoring the second, third, and fourth terms in the right hand side of (3) and solving for least squares estimate for the coarse scale coefficients

$$
\begin{aligned}
f(pr + \epsilon_{i_t}, qr + \epsilon_{i_s}) \quad \approx \quad & \\
\sum_{k,l} a_{J,k,l}\phi_{J,k}(pr + \epsilon_{i_t})&\phi_{J,l}(qr + \epsilon_{i_s}). \quad (4)
\end{aligned}
$$

In matrix form, the sum above can be written as a kronecker product of 1-D wavelet transform matrices

$$
\mathbf{f}^{(i)} \approx (G^{(i)}_{J_t} \otimes G^{(i)}_{J_s})\mathbf{a}_J, \quad i = 1, ..., n, \quad (5)
$$

where $\mathbf{f}^{(i)}$ is the vector with the pixel values of the ith frame reordered rowwise, $\mathbf{a}_J$ is the vector of unknown coarse scale coefficients, and the entries $G^{(i)}_{J_t}, G^{(i)}_{J_s}$ are basis function values at sampling points of frame i along the horizontal and vertical direction, respectively. We solve (5) for a regularized least squares estimate $\hat{\mathbf{a}}_J$ of $\mathbf{a}_J$. The difference between $\mathbf{f}^{(i)}$ and its coarse-scale estimate $(G^{(i)}_{J_t} \otimes G^{(i)}_{J_s})\hat{\mathbf{a}}_J$ can next be used to estimate the horizontal detail coefficients $\mathbf{b}^h_J$

$$
\begin{aligned}
\mathbf{g}^{(i)}_J &= \mathbf{f}^{(i)} - (G^{(i)}_{J_t} \otimes G^{(i)}_{J_s})\hat{\mathbf{a}}_J && (6) \\
&\approx (G^{(i)}_{J_t} \otimes H^{(i)}_{J_s})\mathbf{b}^h_J. && (7)
\end{aligned}
$$

The residual is then used to calculate $\mathbf{b}^v_J$ and $\mathbf{b}^d_J$. We pick the finest scale J so that the number of sample values is more than the number of unknown coefficients in (5) and (7).

Once the coefficient estimates $\hat{\mathbf{a}}_J, \hat{\mathbf{b}}^h_J, \hat{\mathbf{b}}^v_J, \hat{\mathbf{b}}^d_J$ at level J have been determined, we can approximate $f(t,s)$ on the HR grid

$$
\begin{aligned}
\hat{f}_J(t,s) \quad = \quad & \sum_{k,l} \hat{a}_{J,k,l}\phi_{J,k}(t)\phi_{J,l}(s) + \\
& \sum_{k,l} \hat{b}^h_{J,k,l}\psi_{J,k}(t)\phi_{J,l}(s) + \\
& \sum_{k,l} \hat{b}^v_{J,k,l}\phi_{J,k}(t)\psi_{J,l}(s) + \\
& \sum_{k,l} \hat{b}^d_{J,k,l}\psi_{J,k}(t)\psi_{J,l}(s), \quad (8)
\end{aligned}
$$

for $\{(t,s)| \ t = 0, ..., hr-1, \ s = 0, ..., wr-1\}$.

3. COMPUTATIONAL COMPLEXITY

We use the conjugate gradient (CG) iterative method to solve for regularized estimates of the wavelet coefficients. The main computational burden for CG is two matrix-vector products involving the system matrix (cf.

[1]). The system matrix for our 2-D interpolation problem comes from (5) and is a series of kronecker products of 1-D wavelet transform matrices. We recall the following property of the kronecker product

$$(A \otimes B)\text{reshape}(V) = \text{reshape}(AVB^T) \qquad (9)$$

where $\text{reshape}(\cdot)$ reorders the entries of a matrix in rowwise order into vector format. The difference in the main computational cost between the 2-D and 1-D interpolation problems is two matrix multiplications instead of one. So by taking advantage of the interlacing structure and the kronecker product representation, the computational cost for our interpolation approach only doubles for the 2-D case as compared to the 1-D case.

4. WAVELET SUPERRESOLUTION EXPERIMENTS FOR 2-D IMAGES

The low resolution Forward Looking Infrared (FLIR) images in our superresolution experiment are provided courtesy of Brian Yasuda and the FLIR research group in the Sensors Technology Branch, Wright Laboratory, WPAFB, OH. Each image is 64×64 pixels and a resolution enhancement factor of 5 is sought after. The objects in the scene are stationary, and 16 frames are acquired by controlled movements of a FLIR imager described in [4]. Figure 1 contains the results of our wavelet-based superresolution algorithm for the FLIR test sequence using Daubechies DB4 filter interpolation, along with Tikhonov regularized deblurring using an identity regularization matrix.

5. SUMMARY

In this paper, we present a new interpolation-restoration method for image superresolution. In contrast to previous interpolation-restoration approaches, our method exploits the interlacing structure of the sampling grid in superresolution. Using a separable orthonormal wavelet basis for 2-D images, we derive a wavelet decomposition using kronecker products. As a results, the computational properties of the kronecker products allow efficient calculation of the wavelet coeffcients. Computational complexity of our method applied to 2-D interlaced data increases only by a factor of 2 compared to that in 1-D.

6. REFERENCES

[1] O. Axelsson. *Iterative Solution Methods.* Cambridge University Press, New York, NY, 1994.

[2] M. Elad. *Super-resolution Reconstruction of Images.* PhD thesis, The Technion - Israel Institute of Technology, Dec. 1996.

[3] C. Ford and D. Etter. Wavelet basis reconstruction of nonuniformly sampled data. *IEEE Trans. on Circuits and Systems II*, 45(8):1165–1168, Aug. 1998.

[4] R. Hardie, K. Barnard, and E. Armstrong. Joint MAP registration and high-resolution image estimation using a sequence of undersampled images. *IEEE Trans. on Image Processing*, 6(12):1621–1633, Dec. 1997.

[5] S. Mallat. A theory for multiresolution in signal decomposition: The wavelet representation. *IEEE Trans. on Pattern Analysis and Machine Intelligence*, 11(7):674–683, Jul. 1989.

[6] N. Nguyen. *Numerical Techniques for Image Superresolution.* PhD thesis, Stanford University, Apr. 2000.

[7] H. Shekarforoush and R. Chellappa. Data-driven multi-channel super-resolution with application to video sequences. *Journal of the Optical Society of America A*, 16(3):481–492, Mar. 1999.

[8] A. Tekalp, M. Ozkan, and M. Sezan. High-resolution image reconstruction from lower-resolution image sequences and space-varying image restoration. In *Proc. ICASSP '92*, volume 3, pages 169–172, San Francisco, CA, March 1992.

[9] H. Ur and D. Gross. Improved resolution from sub-pixel shifted pictures. *CVGIP: Graphical Models and Image Processing*, 54(2):181–186, Mar. 1992.

Sample LR frame

20

40

60

20   40   60

Coarse scale reconstruction

100

200

300

100   200   300

+ Horizontal detail

100

200

300

100   200   300

+ Vertical detail

100

200

300

100   200   300
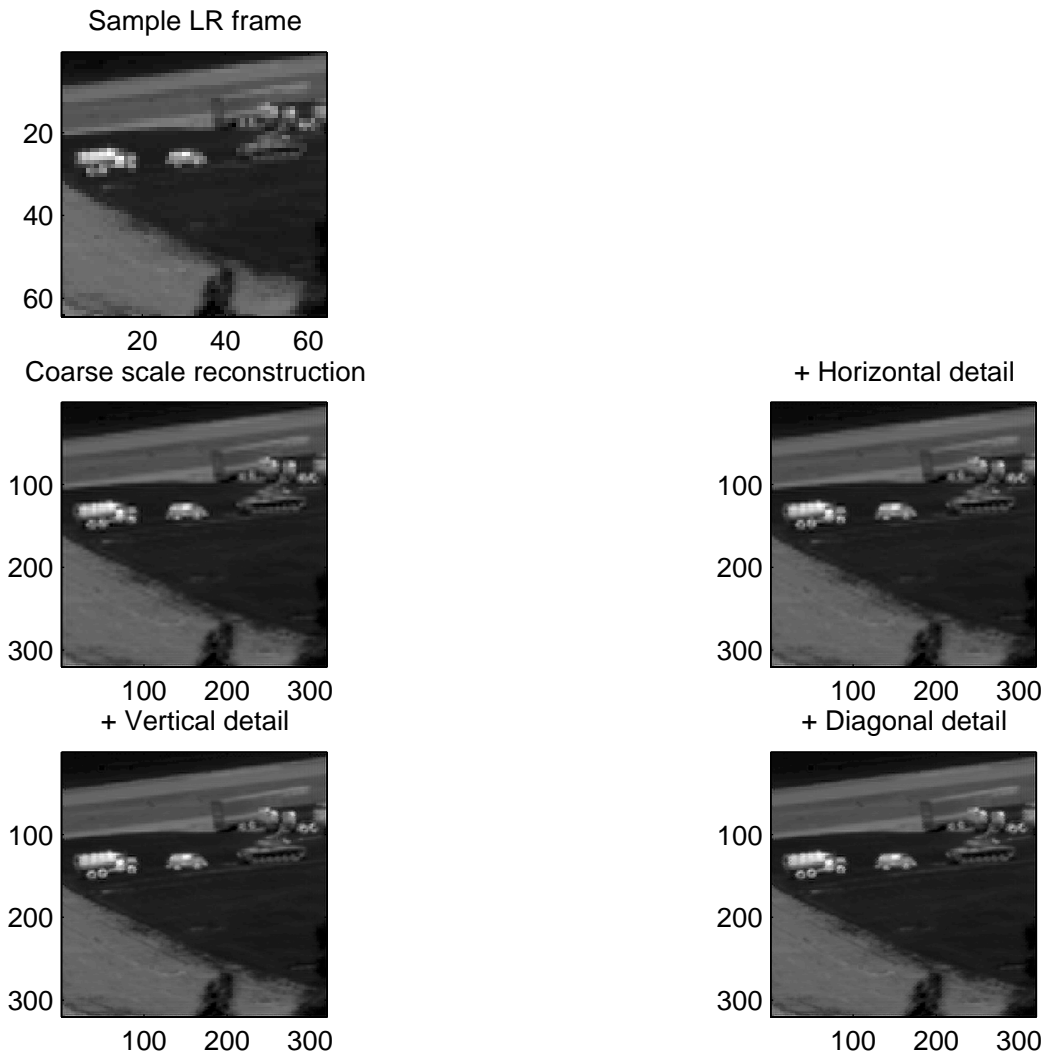
+ Diagonal detail

100

200

300

100   200   300

Figure 2: The first (upper left) display is a sample FLIR LR frame. The subsequent images are the coarse scale approximation plus various incremental levels of detail refinements.